ACS APPLIED MATERIALS & INTERFACES

Research Article

www.acsami.org

Effect of the Duration of UV Irradiation on the Anticoagulant Properties of Titanium Dioxide Films

Jiang Chen, Ping Yang,* Yuzhen Liao, Jinbiao Wang, Huiqing Chen, Hong Sun, and Nan Huang

Institute of Biomaterials and Surface Engineering, Key Laboratory for Advanced Technologies of Materials, Ministry of Education, Southwest Jiaotong University, Chengdu 610031, People's Republic of China

Supporting Information

ABSTRACT: Recently, UV irradiation has been reported as a new approach to significantly improve the anticoagulant properties of titanium dioxide (TiO_2) films by suppressing fibrinogen adsorption and platelet adhesion. This study focuses on how fibrinogen adsorption of and platelet adhesion to TiO_2 films is affected by the duration of UV irradiation. Furthermore, this study intends to describe the link between the suppression effect and the changes in the TiO_2 films nature caused by photogenerated reactive oxygen species (ROS). First, we performed UV irradiation in different atmospheres as model 1 to determine the effect of oxygen gas on the anticoagulant properties of TiO_2 films. The results showed that the suppression of platelet adhesion induced by UV irradiation depended on the presence of oxygen gas, indicating that ROS were photogenerated, and the ROS-induced surface change was related to the improvement in the anticoagulant ability. Then, we fabricated three other types of TiO_2 samples in air by varying the UV irradiation time: (1) model 2, comprising fully UV-irradiated TiO_2 films, (2) model 3, comprising partially UV-irradiated TiO_2 films, and (3) model 4, comprising fully UV-irradiated TiO_2−Si micropatterns. The results indicated that UV irradiation affected the anticoagulant properties of TiO_2 films in a time-dependent manner. UV irradiation on TiO_2 films for short duration (e.g., 1 min) evidenced a suppression effect on fibrinogen adsorption and platelet adhesion, an effect that could not be the result of photoinduced superhydrophilicity, increased hydroxyl groups (−OH) number, or decomposition of the adsorbed hydrocarbon. When the UV irradiation time was longer, this suppression effect extended from the surface of the UV-irradiated TiO_2 films to the surface of the adjacent masked TiO_2 films and the nearby Si surface. This result supported that the suppression effect could be related to the changes in the nature of the TiO_2 films that were caused by the photogenerated and diffused ROS. Further, this extension of the suppression effect to the Si surface indicated that the photogenerated ROS could be used to improve the anticoagulant properties of other materials. A prolonged UV irradiation time (e.g., 240 min) may enhance the fibrinogen adsorption of and platelet adhesion to TiO_2 films, which could be related to the decomposition of the adsorbed hydrocarbon and the increase in the positive charge. However, when comparing the enhancement effect and the suppression effect, the results showed that the latter was the main one to influence fibrinogen adsorption of and platelet adhesion to TiO_2 films. This study provides an important basis for understanding the behavior of UV-irradiated TiO_2 films as anticoagulant materials.

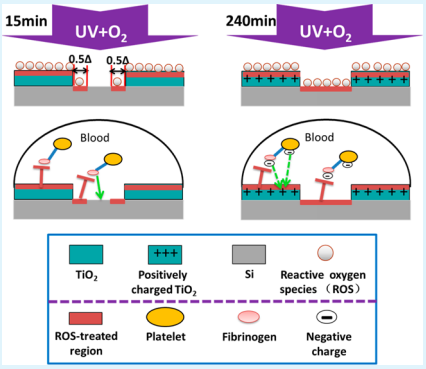

KEYWORDS: *duration of UV irradiation, titanium oxide (TiO_2), micropattern, fibrinogen, platelet*

1. INTRODUCTION

In the past few years, titanium dioxide (TiO_2) films were widely used as biomaterials in various research areas; for instance, they were used in blood contact materials[1] and bone-anchored implants[2] due to their resistance to corrosion and their blood and bone compatibility. Recently, UV irradiation was reported as a facile and efficient method for altering the biocompatibility of TiO_2 films. When TiO_2 films were used as a blood contact material, UV irradiation remarkably improved their anticoagulant ability by suppressing fibrinogen adsorption and conformational change and subsequently inhibiting platelet adhesion and activation.[3] When TiO_2 films were used as bone-anchored implants, UV irradiation was reported to strongly enhance protein adsorption and cell adhesion and thus improve their osteoconductive capacity.[4,5]

From the above studies, UV irradiation seems to provide TiO_2 films with one of two conflicting effects—the suppression effect on fibrinogen (a serum protein) adsorption and platelet (an anuclear cell) adhesion; and the enhancement effect on protein adsorption and cell adhesion. It is interesting to study whether the two effects could coexist and which of these effects prevails on fibrinogen adsorption and platelet adhesion.

Further, while the enhancement effect was demonstrated to be related to the increase in positive charge on the UV-irradiated TiO_2 surfaces,[6,7] the mechanism of the suppression effect on fibrinogen adsorption and platelet adhesion has been

Received: December 22, 2014
Accepted: February 4, 2015
Published: February 13, 2015

ACS Publications © 2015 American Chemical Society

DOI: 10.1021/am509006y
ACS Appl. Mater. Interfaces 2015, 7, 4423−4432

rarely investigated. In our previous study, we showed that after partial UV irradiation, the fibrinogen-dark regions (where fibrinogen adsorption was suppressed) occupied a larger area than the UV-irradiated regions. This extension of the fibrinogen-dark regions was similar to the one evidenced by the organic-oxidized region that was caused by the remote photocatalysis of TiO_2.[3] The extension effect indicated that the suppression effect might be related to the changes in the nature of the TiO_2 surface that are caused by the photogenerated and diffused reactive oxygen species (ROS). If this hypothesis is true, the oxygen gas would contribute to the enhancement of the anticoagulant ability of TiO_2 films, and the size of the extended area of the fibrinogen-dark regions would depend on the duration of UV irradiation, as evidenced by the extension effect of the remote photocatalysis on oxidation of organics.[8] Therefore, it is necessary to determine whether the UV-induced suppression effect depends on the presence of oxygen gas and to study the influence of UV irradiation of varying durations on the extension of the fibrinogen-dark regions. Furthermore, in the study related to the remote photocatalysis, the photogenerated ROS could diffuse from the TiO_2 surface to the nearby surface of the other materials and oxidize the adsorbed organics molecules.[9] However, it was rarely reported whether the suppression effect on fibrinogen adsorption and platelet adhesion could extend in a similar way to the other materials adjacent to the TiO_2 films.

On the other hand, little is known about the way the changes in the nature of the TiO_2 films, produced by the photogenerated ROS, affect fibrinogen adsorption and platelet adhesion. The changes caused by ROS in the nature of the TiO_2 films that might influence the fibrinogen adsorption and platelet adhesion are described in the following sections.

1.1. Retained ROS on the TiO_2 Surface. When TiO_2 films are treated with UV radiation, the separated electron−hole pairs immediately generate ROS.[10−12] Further, many of the photogenerated ROS can influence thrombus formation.[13−16] Moreover, some ROS (e.g., $O_2^{\bullet-}$, HO_2, and H_2O_2) have a relatively long lifetime (ranging from minutes to hours) in air.[17−19] Hence, the retained ROS may influence the blood compatibility of the UV-irradiated TiO_2 films.

1.2. Oxidation of Adsorbed Hydrocarbon. When the TiO_2 films are stored in air, they will inevitably get contaminated by hydrocarbon adsorption.[20] In the course of several minutes of UV irradiation, the photogenerated ROS can induce oxidation of the adsorbed hydrocarbon,[21] which perhaps influences fibrinogen adsorption of and platelet adhesion to these films.

1.3. Photoinduced Superhydrophilicity. It is known that as little as several minutes of UV irradiation can strongly improve the hydrophilicity of TiO_2 films.[22−24] Because the superhydrophilic surface is considered to be beneficial for maintaining protein conformation,[25] the UV-induced superhydrophilic TiO_2 surface may have an effect on the suppression of the conformational change of fibrinogen and subsequently on the inhibition of the adhesion and activation of platelet.

1.4. Increase in Hydroxyl Groups (−OH). The UV irradiation of TiO_2 films lasting for a few minutes to several hours can increase the amount of −OH through the reaction of photogenerated ROS and the adsorbed water molecules.[23,26,27] The surface modified by the increased amount of −OH is usually considered to benefit blood compatibility due to its low affinity for fibrinogen.[28]

1.5. Decomposition of Adsorbed Hydrocarbon. The automatically absorbed hydrocarbon may influence the anticoagulant properties of the TiO_2 films. Upon UV irradiation, some of the photogenerated ROS, such as ·OH, can decompose the adsorbed hydrocarbon into CO_2 and H_2O.[29] Adequate decomposition of hydrocarbon may require several hours.[5] Moreover, the decomposition of the adsorbed hydrocarbon may influence the anticoagulant properties of TiO_2 films.

1.6. Increase in Positive Charge. It was reported that several hours of UV irradiation can turn the TiO_2 surface from negatively to positively charged by the adequate decomposition of the adsorbed hydrocarbon and thus improve the attachment of proteins and cells by means of electrostatic attraction.[6,7] The positively charged surface could be detrimental for the anticoagulant ability, for it may enhance the attachment of fibrinogen and platelets.

As mentioned above, changes in the nature of TiO_2 surface caused by the photogenerated ROS were dependent on the duration of the UV irradiation. This suggested that the anticoagulant properties of TiO_2 films might be dependent on the duration of UV irradiation to which they are subjected, and that the variation of the duration of UV irradiation could be used to investigate the relationship between the changes the nature of the TiO_2 films and the fibrinogen adsorption and platelet adhesion.

It was demonstrated that fibrinogen absorption and platelet adhesion are sensitive to the changes in the TiO_2 surface caused by UV irradiation.[3] Thereby, they could be used as biological probes to detect the change in the anticoagulant property of TiO_2 under different duration of UV irradiation. Micropatterning is a powerful tool to study the remote photocatalysis because it can provide a direct insight on the diffusion of ROS.[8,9,30] Micropatterning is also a popular technology to study the selective attachment of proteins and cells,[31−33] which can be used to investigate both the suppression and enhancement effects on fibrinogen adsorption and platelet adhesion of the UV-irradiated TiO_2 films.

In this study, fibrinogen and platelets were used either together or one at a time as biological probes on the four fabricated models. To produce model 1 samples, we fully UV-irradiated TiO_2 films in different atmospheres for 1 h to study the relationship between the presence of oxygen gas and the UV-induced suppression effect.

To produce model 2 samples, we fully UV-irradiated TiO_2 films in air for various time intervals to determine the relationship between the changes in the nature of TiO_2 films induced by the photogenerated ROS, and the response of fibrinogen adsorption and platelet adhesion were determined. To produce model 3 samples, we partially UV-irradiated TiO_2 films in air for various time intervals in the presence of a photomask to determine the response of the suppression effect and the extension effect. To produce model 4 samples, we fully UV-irradiated TiO_2−Si micropatterns in air for various time intervals to study the suppression, extension, and enhancement effect on the same model. Furthermore, we used model 4 to investigate whether the extension effect applies to the other materials nearby TiO_2.

2. MATERIALS AND METHODS

2.1. Materials and UV Irradiation Treatment. Anatase TiO_2 films were fabricated on the Si substrate by using a magnetron sputtering deposition system. The parameters of deposition is given in

DOI: 10.1021/am509006y
ACS Appl. Mater. Interfaces 2015, 7, 4423−4432

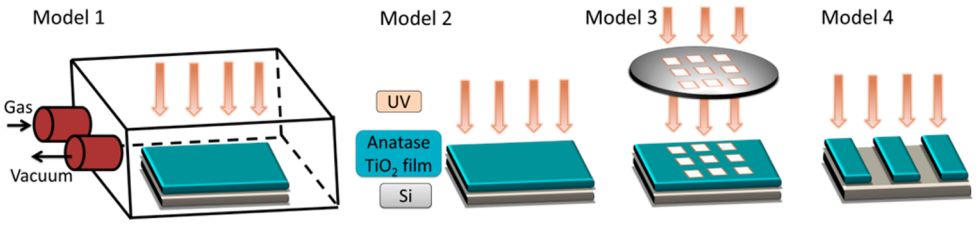

Figure 1. Strategies for the fabrication of the four models.

Table S1 (Supporting Information). TiO_2−Si micropatterns were fabricated on the Si substrate by using a magnetron sputtering deposition system and a lithography machine (Chinese Academy of Sciences, China). The fabrication process of TiO_2−Si micropattern is given in Figure S1 (Supporting Information).

The TiO_2−Si micropatterns consisting of alternating stripes of TiO_2 and Si were represented as mla−b ("a" and "b" represent the width (μm) of TiO_2 stripe and Si stripe, respectively). Six types of TiO_2−Si micropattern were fabricated, including ml10−5, ml10−10, ml10−20, ml20−10, ml40−20, and ml60−30.

All the fabricated samples were stored in air for 8 weeks before UV irradiation and subsequent tests.

The UV irradiation treatments to obtain the four models are displayed in Figure 1. In model 1, the anatase TiO_2 films were fully UV-irradiated for 1 h in different atmospheres in glass boxes, including vacuum (vacuum pressure: 5000 Pa), air, and oxygen gas (gas pressure: 0.11 MPa). In model 2, the TiO_2 films were fully UV-irradiated in air for various times, including 0, 1, 10, 30, 60, 120, and 240 min. In model 3, the TiO_2 films were partially UV-irradiated in air in the presence of a photomask (with transparent squares 25 μm on a side separated by 25 μm intervals) for various times, including 0, 1, 10, 30, and 120 min. In model 4, the TiO_2−Si micropatterns were fully UV-irradiated in air for various times, including 0, 15, 30, 60, 120, and 240 min. All UV irradiation treatments were performed by a lithography machine (Chinese Academy of Sciences, China) with UV light intensity of 16 mW/cm^2 (λ = 365 nm).

After UV irradiation, the samples were stored in air for 15 min before biological testing and hydrophilic testing, in air for 15 min and in vacuum (2×10^{-7} mB) for 12 h before the X-ray photoelectron spectroscopy (XPS) testing, and in air for 12 h before the surface charge testing.

2.2. Characterization of TiO_2 Films. The structures of TiO_2 films were determined by X-ray diffraction (XRD; X'Pert Pro MPD, Philips, Holland) by using a copper target at a glancing angle of 0.5°. The hydrophilicity of TiO_2 films was examined using a drop shape analysis system (DSA 100, Krüss, Germany) by the sessile drop method (5 μL droplet). The surface compositions of the films were detected by the X-ray photoelectron spectroscopy (XPS; XSAM800, Kratos, Ltd., United Kingdom), and the instrument was equipped with a monochromatic Al Kα (1486.6 eV) X-ray source operated at 12 kV × 15 mA at a pressure of 2×10^{-10} mB. The C 1s peak at 284.8 eV was used as a reference for charge correction. The surface charge of TiO_2 films (18 × 18 mm) were examined by EST111 Static Charge Meter (EST Electro-Static Test Co., Ltd., China) in air.

2.3. Characterization of TiO_2−Si Micropatterns. The TiO_2−Si micropatterns surface topography were detected by scanning electron microscope (SEM; Quanta 200, FEI, Holland) and surface profiler (Ambios XP-2, Ambios, Santa Cruz, CA). The element distribution on the surface was analyzed by energy dispersive spectroscopy (EDS; Quanta 200, FEI, Holland). The structures of TiO_2 were determined by XRD in the same way described in chapter 2.2.

2.4. Platelet Adhesion. Fresh venous blood obtained from a healthy adult volunteer was centrifuged at 1500 rpm for 15 min to obtain platelet-rich plasma (PRP). Then, the samples (7 × 7 mm^2) were immersed in 350 μL of PRP and incubated at 37 °C for 1 h. Subsequently, the samples were rinsed thoroughly with phosphate-buffered saline (PBS) three times to remove nonadhering platelets and were then fixed with 2.5% glutaraldehyde in saline solution for 4 h. Finally, the samples were dried in a CO_2 critical point dryer (CPD030, Bal-Tec AG, Germany) after dehydration and dealcoholization. The samples were observed under an optical microscope (OM; DM4000M, Leica, Germany) and a scanning electron microscope (Quanta 200, FEI, Holland). Twelve OM images with the size of 640 × 480 μm were collected per sample for the analysis of platelets surface coverage (S_p) and platelets density by using ImageJ software (National Institutes of Health, New York.).

2.5. Fibrinogen (Fgn) Adsorption. To examine the occurrence of Fgn adsorption, we covered the TiO_2 samples (7 × 7 mm) with 40 μL of fresh human platelet-poor plasma (PPP) extracted from fresh venous blood obtained from a healthy adult volunteer, which was centrifuged at 3000 rpm for 15 min and incubated at 37 °C for 1 h. After incubation with PPP, the samples were rinsed thoroughly with PBS and blocked with 1 wt % bovine serum albumin (BSA) in PBS at 37 °C for 30 min. Subsequently, the samples were thoroughly washed again and covered with 20 μL of Horseradish Peroxidase (HRP)-labeled mouse antihuman fibrinogen monoclonal antibody (primary antibody, diluted 1:200 in PBS; Sigma, St. Louis, MO) and incubated at 37 °C for 1 h. The samples were thoroughly washed with PBS, following which, 70 μL of chromogenic substrate 3,3′,5,5′-tetramethylbenzidine (TMB) solution (diluted 1:4 in PBS) was added to react with the sample surface. After 10 min, 50 μL of 1 M H_2SO_4 was used to stop the reaction, and the optical density at 450 nm was determined by a microplate reader. The relative amount of adsorbed Fgn was quantified according to the calibration curve.

2.6. Distribution of Adsorbed Fibrinogen. After incubation with PPP at 37 °C for 1 h, the samples (7 × 7 mm) were rinsed three times with PBS to remove nonadhering Fgn. Subsequently, the samples were blocked with 1 wt % BSA in PBS at 37 °C for 30 min and then rinsed with PBS. Finally, FITC-labeled antihuman fibrinogen (Bioss, China) was added and incubated at 37 °C for 1 h. After rinsing with PBS again, the stained samples were observed under an inverted fluorescence microscope (IX51, Olympus, Japan). The green fluorescent intensity of samples were analyzed by the Image Pro Plus software (Media Cybernetics, Rockville, MD). To obtain the relative fluorescent intensity of a fibrinogen-dark square, we divided the fluorescent intensity of one circular area (d = 3 μm) that was identified in the center of the fibrinogen-dark square by the average fluorescent intensity of four circular areas (d = 3 μm) identified in the adjacent fibrinogen-bright regions. The average value of the four fibrinogen-dark squares was considered as the relative fluorescent intensity of the fibrinogen-dark region of the sample.

2.7. Statistics. All the experiments were done in triplicate (n = 3). The statistical significance between the sample groups was assessed by SPSS11.5 software using one-way ANOVA and LSD posthoc test. A value of $p < 0.05$ was considered statistically significant.

3. RESULTS AND DISCUSSION

3.1. Effect of Different Atmospheres on the UV-Induced Anticoagulant Properties (Model 1). *3.1.1. Hydrophilicity and Platelet Adhesion on TiO_2 Films Treated with UV Irradiation in Different Atmospheres.* All the peaks in the XRD spectrum could be attributed to anatase TiO_2, indicating the formation of anatase TiO_2 films on the Si wafer (Figure 2D).

The water contact angle (θ_w) of the untreated TiO_2 film was about 83.6°. After 1 h of UV irradiation in vacuum (vacuum

DOI: 10.1021/am509006y
ACS Appl. Mater. Interfaces 2015, 7, 4423−4432

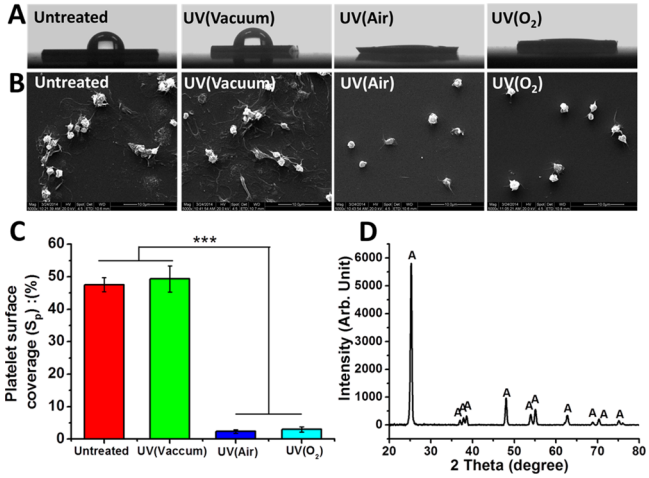

Figure 2. (A) Hydrophilicity, (B) platelet adhesion, and (C) platelet surface coverage on TiO_2 films treated with 1 h of UV irradiation in different atmospheres. (D) Structure of TiO_2 films characterized by XRD.

pressure: 5000 Pa), the θ_w value of the TiO_2 film was about 82.3°, whereas after 1 h of UV irradiation in air and in oxygen, the θ_w value of the films decreased to less than 5° (Figure 2A).

On the untreated TiO_2 films, most of the adhered platelets were spread out and fully activated, leading to aggregation. The adhesion behavior of platelets was not changed significantly by UV irradiation in vacuum for 1 h. However, 1 h of UV irradiation in air and in oxygen gas (gas pressure: 0.11 MPa) both strongly suppressed the adhesion and spreading of platelets on the TiO_2 films (Figure 2B).

The platelet surface coverage (S_p) was analyzed using ImageJ software. On the untreated TiO_2 films, S_p was about 46%, and UV irradiation in vacuum for 1 h did not change this value significantly. However, after 1 h of UV irradiation in air and in oxygen, S_p decreased to about 2.3 and 3.0%, respectively, demonstrating strong suppression of platelet adhesion and spreading (Figure 2C).

3.1.2. Discussion. In model 1, we demonstrated that the suppression of platelet adhesion on the UV-irradiated TiO_2 film depended on the presence of oxygen gas. As is well-known, under an oxygen atmosphere, UV-excited electrons can reacted with O_2 to form $O_2^{\bullet-}$, which can change to other types of ROS such as HO_2 and H_2O_2[34] and change the nature of the TiO_2 surface. In this context, the results in Figure 2 indicate that the photogenerated ROS and ROS-induced surface changes could be related to the enhancement of the anticoagulant ability of the TiO_2 film.

Therefore, in the next model (model 2), we further detected the relationship between the ROS-induced changes in the properties of the TiO_2 surface (including the hydrophilicity, presence of −OH groups, presence of adsorbed hydrocarbons, and surface charge) and the platelet adhesion and fibrinogen adsorption behavior.

3.2. Difference in Fibrinogen Adsorption and Platelet Adhesion on TiO_2 Films Treated with UV Irradiation for Different Durations in Air (Model 2). *3.2.1. Characterization of the TiO_2 Films Subjected to UV Irradiation for Different Durations.* The water contact angle (θ_w) of the untreated TiO_2 films was about 54.5°. After 1, 10, 30, 60, 120, and 240 min of UV irradiation, the θ_w of TiO_2 film decreased to about 29.3°, 5.6°, 3.2°, 2.2°, 1.5°, and 1.5°, respectively (Figure 3A). It is worth noting that after 1 min of UV irradiation, the TiO_2 film became more hydrophilic even if it did not reach the superhydrophilic state.

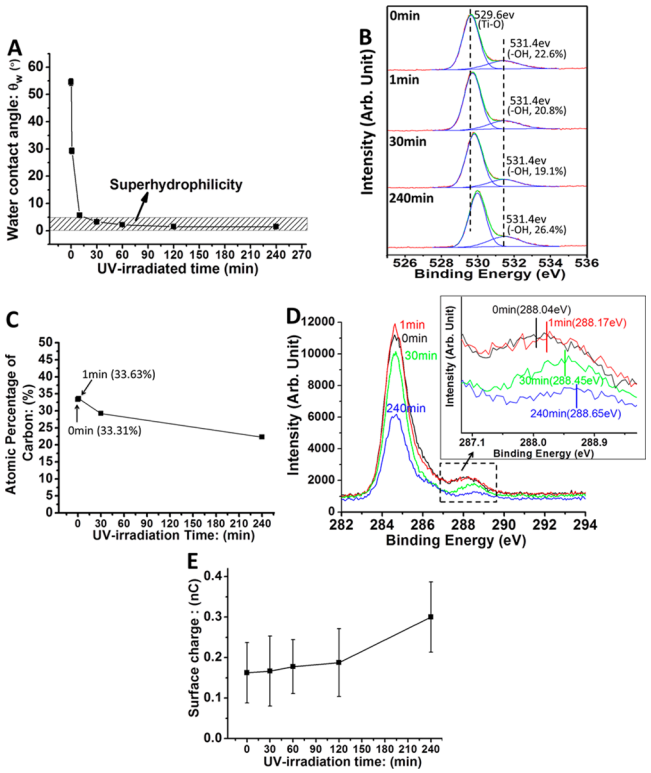

Figure 3. Changes of TiO_2 films after various times of UV irradiation: (A) the water contact angle (θ_w), (B) the close-up view of the XPS O 1s peak, (C) the atomic percentage of carbon, (D) the close-up view of the C 1s peak, and (E) the surface charge.

The changes in the surface composition were analyzed by XPS. Close examination of the O 1s spectrum (Figure 3B) clearly showed two kinds of oxygen with binding energies of about 530 and 531.4 eV, which could be assigned to the Ti−O bonds and −OH groups, respectively.[23,35,36] The atomic percentage of −OH groups in the TiO_2 film without UV irradiation was 22.6%, which decreased to 20.8% after UV irradiation for 1 min, and 19.1% after UV irradiation for 30 min. However, it increased to 26.4% when the irradiation time was 240 min. The atomic percentages of carbon in the TiO_2 films tend to decrease with increasing durations of UV irradiation (Figure 3C). When TiO_2 films were UV irradiated for 0, 1, 30, and 240 min, the atomic percentage of carbon was about 33.31, 33.63, 29.24, and 22.28%, respectively. Close examination of the C 1s peaks (Figure 3D) revealed that the shoulder peaks appeared at about 288 eV and decreased with increasing UV irradiation time, which were attributed to the presence of oxygen-containing hydrocarbons,[20,37]. Additionally, the shoulder peaks shifted to a higher bonding energy when the UV irradiation time was increased (Figure 3D, embedded box). When TiO_2 films were UV-irradiated for 0, 1, 30, and 240 min, the shoulder peaks were at about 288.04, 288.17, 288.45, and 288.65 eV respectively.

The surface charge of the untreated TiO_2 was about 0.16 nC (Figure 3E). When TiO_2 films were UV-irradiated for 30, 60, and 120 min, their surface charge seemed to increase slightly, even if not significantly. However, after 240 min of UV

DOI: 10.1021/am509006y
ACS Appl. Mater. Interfaces 2015, 7, 4423−4432

irradiation, the surface charge of the TiO_2 films increased significantly to about 0.3 nC. (The statistical significance of the differences between the samples was analyzed using the one-way ANOVA and LSD posthoc test.)

3.2.2. Platelet Adhesion and Fibrinogen Adsorption. The shapes of the adhered platelets are presented in Figure 4A. The

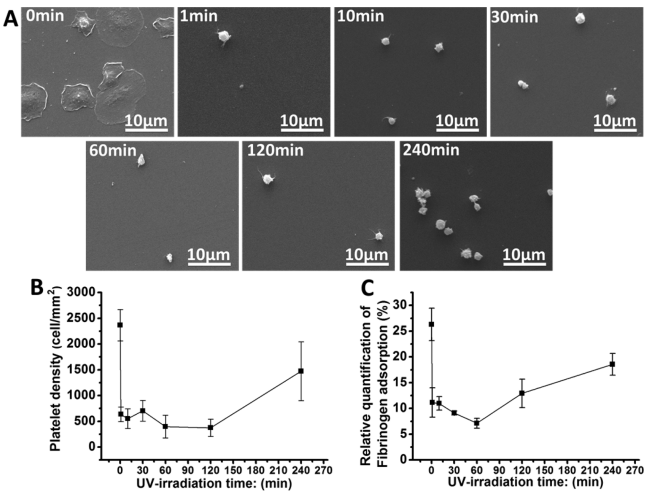

Figure 4. (A) Platelets adhesion, (B) platelets density, and (C) fibrinogen adsorption on the anatase TiO_2 films with various times of UV irradiation.

adhered platelets on the TiO_2 films subjected to 0 min of UV irradiation were spreading out and were fully activated. On the TiO_2 film subjected to UV irradiation for 1 min, the platelet activation was strongly inhibited, since most of the platelets maintained a spherical shape and few cells extended pseudopodia. The platelet activation was also inhibited on the other films subjected to UV irradiation for longer time durations, while the platelets seemed to be slightly aggregated on the TiO_2 films subjected to 240 min of UV irradiation. The platelet adhesion on TiO_2 films was analyzed by ImageJ software (Figure 4B). On the untreated TiO_2 films, the platelet density was about 2360 cells/mm^2, and it significantly decreased to about 640 cells/mm^2 on the 1 min UV-irradiated TiO_2 film. On the TiO_2 films subjected to 10, 30, 60, and 120 min of UV irradiation, the platelet density was about 550, 700, 400, and 370 cells/mm^2, respectively. However, when the UV irradiation time was prolonged to 240 min, the platelet adhesion significantly increased to about 1470 cells/mm^2. The results showed that the platelets density decreased sharply when TiO_2 films were UV-irradiated for a short time (e.g., 1 min), while it relatively increased when the UV irradiation time was long enough (e.g., 240 min). The adsorption of fibrinogen shared the similar "decreasing-increasing" trend when the UV irradiation time was increased (Figure 4C). On the untreated TiO_2 films, the value of the relative quantification of fibrinogen adsorption was about 26.3%. When TiO_2 films were UV-irradiated for 1, 10, 30, and 60 min, fibrinogen adsorption kept decreasing to about 11.1, 11.0, 9.1, and 7.1%, respectively. However, when the UV irradiation time was increased to 120 and 240 min, fibrinogen adsorption significantly increased to 12.9 and 18.6%, respectively. The statistical significance of the differences between the samples was analyzed using the one-way ANOVA and LSD posthoc test.

3.2.3. Discussion. Results showed that the changes in the nature of TiO_2 surface depending on the UV irradiation time. On the other hand, after a short time of UV irradiation (e.g., 1 min) of TiO_2 films, the fibrinogen adsorption and platelet adhesion were suppressed, indicating the development of a suppression effect. When the UV irradiation time was long enough (e.g., 120 min for fibrinogen and 240 min for platelets), fibrinogen adsorption and platelet adhesion relatively increased, indicating the appearance of an enhancement effect.

The relationship between the suppression/enhancement effect and the changes in the nature of TiO_2 films caused by the photogenerated ROS are discussed below.

Effect of Photoinduced Superhydrophilicity. It was reported that platelet adsorption and fibrinogen adhesion were suppressed on the superhydrophilic surface ($\theta_w < 5°$).[38] In this study, the θ_w of the untreated TiO_2 films was about 54.5°, and decreased to about 29.3° after 1 min of UV irradiation (Figure 3A). Meanwhile, both fibrinogen adsorption and platelet adhesion were strongly suppressed (Figure 4). After 10 min of UV irradiation, the θ_w continued to decrease from 29.3 to 5.6° (Figure 3A). However, the behavior of fibrinogen adsorption and platelet adhesion/spreading made no significant difference when compared to that of the 1 min UV-irradiated TiO_2 films (Figure 4). These results indicated that the suppression effect on fibrinogen adsorption and platelet adhesion was not mainly caused by the superhydrophilic state of the UV-irradiated TiO_2 films. Further research is needed to determine the underlying reasons for the appearance of the suppression effect on a moderately hydrophilic TiO_2 surface.

On the other hand, although θ_w for the 60 and 240 min UV-irradiated TiO_2 films were roughly identical (Figure 3A), both fibrinogen adsorption and platelet adhesion increased on the 240 min UV-irradiated TiO_2 film (Figure 4), which indicated that this relative enhancement effect on fibrinogen adsorption and platelet adhesion was unlikely caused by the superhydrophilic state of TiO_2 surface.

Effect of −OH Groups. Some studies reported that the surface modified with −OH groups may suppress fibrinogen adsorption and platelet adhesion.[28] However, Takemoto et al. reported that the Ti surface was rich in −OH groups after treating it with hydrogen peroxide, which did not suppress platelet adhesion.[39] Results showed that, compared to the untreated TiO_2 surface, the atomic percentage of −OH groups on the TiO_2 films that were UV-irradiated for 1 and 30 min decreased (Figure 3B), while platelet adhesion and fibrinogen adsorption were suppressed (Figure 4). These results indicated that the suppression effect on fibrinogen and platelets could not be induced by the increase of the −OH groups on the UV-irradiated films. The results were consistent with those reported by Takemoto et al.[39]

Effect of Hydrocarbon Decomposing. The atomic percentage of carbon and the height of the C 1s peak for the 1 min UV-irradiated TiO_2 films showed no downtrend compared with the untreated TiO_2 films (Figure 3C,D). These results indicate that the decomposing of hydrocarbon could take place below the detection limit of the XPS. Furthermore, fibrinogen adsorption and platelet adhesion levels decreased significantly (Figure 4). Compared with the 1 min UV-irradiated TiO_2 films, hydrocarbon decomposition was detected on the 30 min UV-irradiated TiO_2 films (Figure 3C,D) while the significant changes in fibrinogen adsorption and platelet adhesion were not observed (Figure 4). These results indicated that the decomposition of hydrocarbon could not explain the suppression effect.

DOI: 10.1021/am509006y
ACS Appl. Mater. Interfaces 2015, 7, 4423−4432

On the other hand, after 240 min of UV irradiation, the hydrocarbon decomposed significantly (Figure 3C,D), which could be related to the increase in the surface charge. Moreover, this decomposition could have an enhancement effect on fibrinogen adsorption and platelet adhesion (Figure 4).[6,20]

Effect of Hydrocarbon Oxidation. It was reported that several minutes of UV irradiation could oxidize adsorbed hydrocarbons such as acetone and acetic acid on anatase TiO_2 to form an asymmetric coordinated end-on Ti−O−C═O structure, which was a stable intermediate with large residues after 60 min of UV illumination.[21] In this manuscript, the C 1s shoulder peak of the untreated TiO_2 film at 288.04 eV could be assigned to the Ti−O−C structure.[40,41] After UV irradiation, the shoulder peak continued to shift to higher binding energies, indicating the oxidation of adsorbed hydrocarbons, which may be induced by the oxidation of some of the Ti−O−C structure to form the Ti−O−C═O structure (with a bonding energy of about 289.3 eV[42]). It is worth noting that both the oxidation of the adsorbed hydrocarbons and the suppression effect appeared to be sensitive to UV irradiation. After 1 min of UV irradiation, the shoulder peak shifted from 288.04 to 288.17 eV, and the fibrinogen adsorption and platelet adhesion were suppressed. Therefore, it is interesting to further study the connection between the oxidization of hydrocarbon adsorbates and the suppression effect.

Effect of Surface Charge. After 240 min of UV irradiation, the surface charge of the TiO_2 films increased significantly (Figure 3E), which could be influenced by the hydrocarbon decomposition.[6,7] This surface charge increase might be responsible for the enhancement effect on platelet adhesion and fibrinogen adsorption (Figure 4), for cells and proteins in the blood are usually negatively charged.[6,7] Additionally, after 240 min of UV irradiation, fibrinogen adsorption and platelet adhesion of TiO_2 films was relatively higher compared with the 60 min UV-irradiated TiO_2 films; however, the values were still lower than those for the untreated TiO_2 films. Furthermore, the platelet spreading on the 240 min UV-irradiated TiO_2 films was still inhibited (Figure 4). These additional results indicated that the suppression effect may have a regulatory role in determining the response of platelet adhesion and fibrinogen adsorption, superseding the enhancement effect.

The present results indicate that a short UV irradiation time (e.g., 1 min) suppressed the fibrinogen adsorption and platelet adhesion, which could not be the result of photoinduced superhydrophilicity, increased hydroxyl groups (−OH) number, or decomposition of the adsorbed hydrocarbon. More efforts should be made to study the other changed natures of the UV-irradiated TiO_2 films (e.g., the retained ROS and the oxidized hydrocarbon) to further explore the underlying mechanisms of the suppression effect. On the other hand, prolonged UV irradiation (e.g., for 240 min) may enhance the fibrinogen adsorption of and platelet adhesion to TiO_2 films, which could be related to the decomposition of the adsorbed hydrocarbons and the increase in the positive charge.

3.3. Change in Fibrinogen Adsorption on TiO_2 Films Depending on Duration of Partial UV Irradiation (Model 3). *3.3.1. Changes in Fibrinogen Adsorption.* The results obtained for model 1 supported the hypothesis that the suppression effect was related to the photogenerated ROS. If this hypothesis is true, the size of the fibrinogen-dark region under partial UV irradiation would increase when the duration of the UV irradiation increased. The results obtained for model 2 demonstrated that fibrinogen adsorption on the TiO_2 films showed a decreasing-increasing trend when the UV irradiation time was increased. Partial UV irradiation may provide direct insight on the decreasing-increasing trend. Therefore, it would be useful to study the change in fibrinogen adsorption on TiO_2 films under partial UV irradiation for different durations.

The fibrinogen-dark squares (where fibrinogen adsorption was suppressed) were observed on the partially UV-irradiated TiO_2 surface (Figure 5A). When the films were subjected to

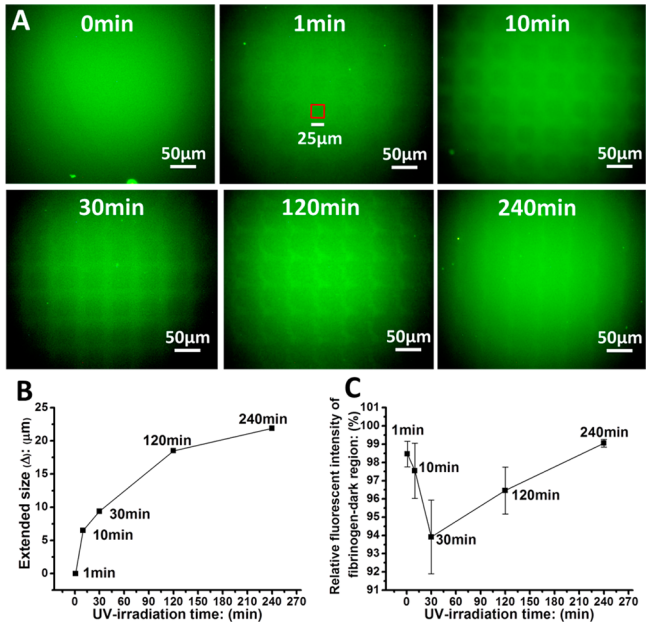

Figure 5. (A) Extension of the fibrinogen-dark square versus the duration of UV irradiation. (B) The extend size of squares versus the duration of UV irradiation. (C) The relative fluorescent intensity of fibrinogen-dark squares.

partial UV irradiation for 1 min, the squares were dim, and their side-length was approximately 25 μm, corresponding with the UV-irradiated region. When the duration of UV irradiation was increased, the squares became clearer and wider. However, when the duration of UV irradiation was 240 min, the squares were largest in size and appeared to be dimmer again. After 10, 30, 120, and 240 min of UV irradiation, the value of Δ was about 6.5, 9.4, 18.5, and 21.9 μm respectively (Figure 5B). The relative fluorescent intensity of fibrinogen-dark regions constantly decreased from about 98.5 to about 94.0% with increasing durations of UV irradiation (from 1 to 30 min). Further, when the duration of UV irradiation increased from 30 to 240 min the relative fluorescent intensity increased from about 94.0 to about 99.0%. These results evidenced a decreasing-increasing trend with increasing UV irradiation time (Figure 5C).

3.3.2. Discussion. The fibrinogen-dark squares were formed after a short time of UV irradiation (1 min), indicating the appearance of the suppression effect on fibrinogen adsorption. With increasing duration of UV irradiation, the dark squares of fibrinogen extended, indicating that the suppression effect was spreading to the adjacent areas. The characteristics of the suppression effect (to extend and be "fast") were reminiscent of the photogenerated ROS characterized by a diffusion ability. This results supported the hypothesis that the suppression effect of fibrinogen adsorption could be related to the change of the TiO_2 surface nature caused by the photogenerated and

DOI: 10.1021/am509006y
ACS Appl. Mater. Interfaces 2015, 7, 4423−4432

diffused ROS (Figure 5C). On the other hand, the relative fluorescent intensity of the fibrinogen-dark regions, showed a decreasing-increasing trend when the UV irradiation time increased (Figure 5E). This result indicated that the adsorption of fibrinogen decreased first, followed by an increase that was dependent on the duration of the UV irradiation. Additionally, this upward trend may indicate the appearance of an enhancement effect on fibrinogen adsorption.

On the other hand, protein patterning is useful for many applications, such as patterning cells. We reported previously that fibrinogen and platelets can be patterned easily on TiO_2 films using partial UV irradiation.[3] However, for protein micropattern fabrication, the fibrinogen-dark region should correspond to the UV-irradiated region (namely, the transparent region on the photomask), and have a strong suppression effect on fibrinogen adsorption. The results obtained for model 3 showed that a short period (e.g., 1 min) of partial UV irradiation can be used to fabricate a fibrinogen-dark region with relatively high precision, whereas the suppression effect was relatively weak. A relatively long period (e.g., 30 min) of partial UV irradiation can strongly suppress the adsorption of fibrinogen, and the fibrinogen-dark region was obviously extended (Figure 5B,C). Therefore, an adequate irradiation time intermediate between the short period and the relatively long period is suggested for fabricating fibrinogen micropatterns on TiO_2 films using partial UV irradiation.

3.4. Adhesion Behavior of Platelets on TiO_2–Si Micropatterns Subjected to UV Irradiation for Different Times (Model 4).

From the two models above, UV irradiation seems likely to provide TiO_2 films with the effects such as suppression, extension, and enhancement. Using model 4, we studied these effects together, which may prove valuable for a better understanding of TiO_2 films as an anticoagulant material.

3.4.1. Characterization of TiO_2–Si Micropatterns. We fabricated various TiO_2–Si micropatterns (ml10–5, ml10–10, ml10–20, ml20–10, ml40–20, and ml60–30). The ml20–10 was representative for SEM, EDS, surface profiler, and XRD analyses. The SEM, EDS, and surface profiler results for the ml20–10 (Figure 6A) showed that the intensity peaks of Ti

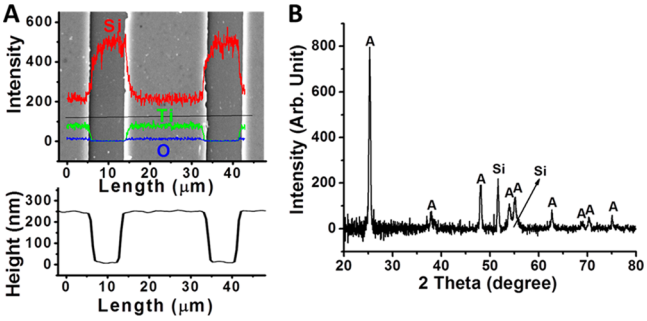

Figure 6. (A) Morphology, element distribution, and height of ml20–10. (B) The structure of TiO_2 in ml20–10 characterized by XRD.

and O were observed on the line with 20 μm in width and 250 nm in height, indicating that TiO_2 stripes with 20 μm in width and 250 nm in height were fabricated. The intensity peak of Si was found on the stripes 10 μm in width, indicating the exposure of Si. The XRD result indicated that the crystal structure of the TiO_2 stripes was anatase (Figure 6B), and that the Si substratum was exposed.

3.4.2. Adhesion Behavior of Platelets on Fully UV-Irradiated TiO_2–Si Micropatterns. Figure 7A shows evidence

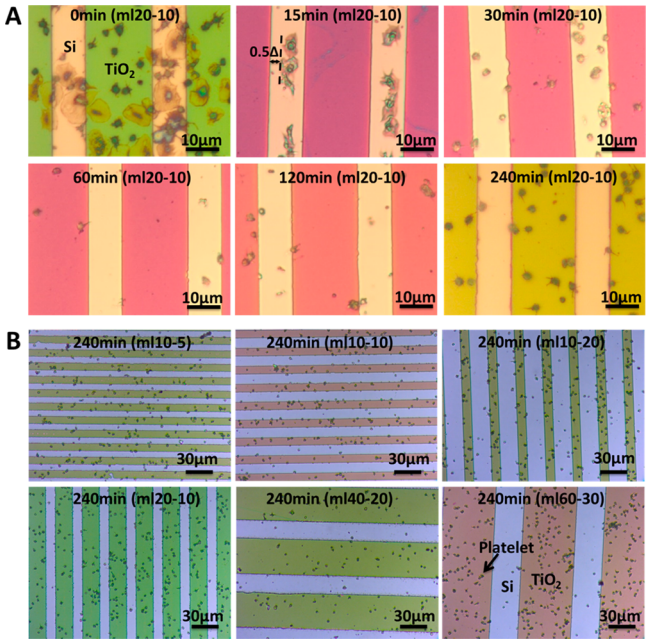

Figure 7. (A) Platelet adhesion on ml20–10 with the various times of UV irradiation, (B) platelets selectively adhered to TiO_2 region on the TiO_2–Si micropatterns which were UV-irradiated for 240 min.

that the platelet adhesion behavior on ml20–10 after the micropatterns were UV-irradiated for various time intervals. When ml20–10 was UV-irradiated for 0 min, the platelets adhered and spread randomly on the TiO_2–Si micropattern. In particular, the platelets membranes could spread across the boundary between the Si regions and TiO_2 regions. The height of 250 nm between the regions of Si and TiO_2 appeared not to restrict the shape of the platelets. When ml20–10 was UV-irradiated for 15 min, the adhesion and spreading of platelets on the TiO_2 regions were strongly inhibited. Platelets selectively adhered and spread on the Si regions, and the membranes of the spread platelets maintained distance from the TiO_2 regions. These results indicated that the suppressed effect of platelets spreading extended from the TiO_2 regions to the nearby Si regions, for UV irradiation is generally considered to not change the nature of Si. We defined the distance between the spread platelets and the TiO_2 regions as 0.5Δ. When the UV-irradiated time prolonged to 30 min, platelets still tended to adhere to the Si regions, while their spreading was suppressed, suggesting that the suppression effect was extended from the TiO_2 regions to the entire Si regions. The platelet adhesion on the Si regions kept decreasing with the increase in the duration of UV irradiation. When the duration of UV irradiation was 60 min, few platelets adhered on both Si and TiO_2 regions. However, the UV irradiation for 120 min appeared to slightly increase the platelet adhesion on the TiO_2 regions, while the adhesion of platelets on the Si regions was still prevented. As for the results from the 240 min UV-irradiated TiO_2–Si micropattern, the platelets were found to be selective when adhering to the TiO_2 regions for the adhesion of platelets increased significantly on the TiO_2 region while it was inhibited on the Si region.

Past results showed that the two-dimensional size of micropatterns may affect the adhesion behavior of the cells,

DOI: 10.1021/am509006y
ACS Appl. Mater. Interfaces 2015, 7, 4423–4432

for example, there may exist a threshold ligand adsorption size necessary to facilitate platelet adhesion and spreading.[43] However, in this study, the platelets evidenced selective adhesion to the TiO_2 region on all the 240 min UV-irradiated micropatterns despite the size differences (Figure 7B). This result indicated that the selective adhesion of platelets was not mainly affected by the two-dimensional size of the UV-irradiated TiO_2−Si micropatterns.

The extension effect of the suppressed region of the platelets spreading was examined by measuring the value of 0.5Δ on the edge of the ml20−10 (Figure 8A). The value of the 0.5Δ increased with increasing durations of UV irradiation. When the ml20−10 was UV-irradiated for 0, 15, 30, 60, 120, and 240 min, the value of 0.5Δ was about 0, 1.4, 3.0, 9.5, 22.4, and 27.5 μm, respectively (Figure 8B). Additionally, when platelets had higher activity, the extension effect could be observed more clearly, e.g. on the ml10−5 with 0 and 120 min of UV irradiation (Figure 8C,D).

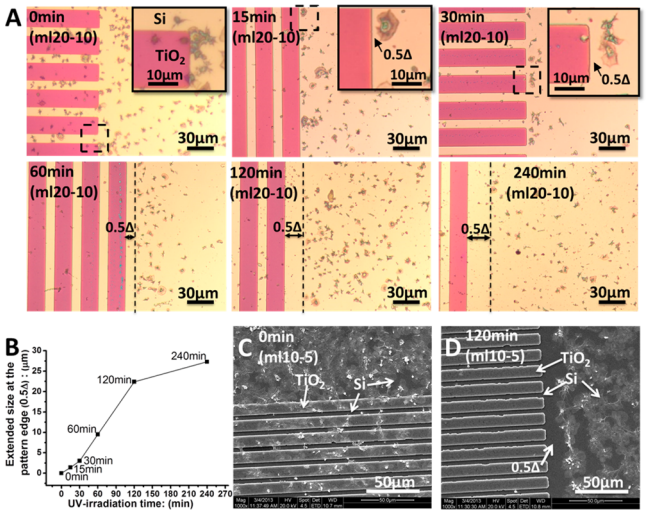

Figure 8. (A) Extension of the platelets spreading suppressed region versus the UV irradiation time. (B) The extend size at the pattern edge (0.5Δ) versus the UV irradiation time. Platelets adhesion and spreading on the (C) 0 min and (D) 120 min UV-irradiated ml10−5.

3.4.3. Discussion. It is interesting to observe that the suppression effect on the platelet adhesion extended from the TiO_2 region to the Si region. The extension distance increased with increasing UV irradiation time, behavior that was reminiscent of the remote photocatalysis. The results supported the hypothesis that the suppression effect of the UV-irradiated TiO_2 on fibrinogen adsorption and platelet adhesion could be related to the changes in the TiO_2 surface nature caused by the photogenerated and diffused ROS. Additionally, the results are important for potential applications because they indicated that the photogenerated ROS of the TiO_2 films can change the nature of other materials (e.g., Si) and thus suppress the platelet adhesion, which may provide a new approach to improve other materials anticoagulant properties. Finally, the UV irradiation time dependent effects of TiO_2 films on the behavior of fibrinogen adsorption and platelet adhesion, including the suppression effect, extension effect and enhancement effect, were shown in model 3. In this part of the study, we classified the behaviors of the platelet adhesion into four representative types. Further, the proposed mechanism of the four types of platelet adhesion behavior is schematically presented in Figure 9.

(1) The TiO_2−Si micropattern was UV-irradiated for 0 min. When the TiO_2−Si micropattern made contact with the blood, the fibrinogen was randomly adsorbed on the TiO_2−Si

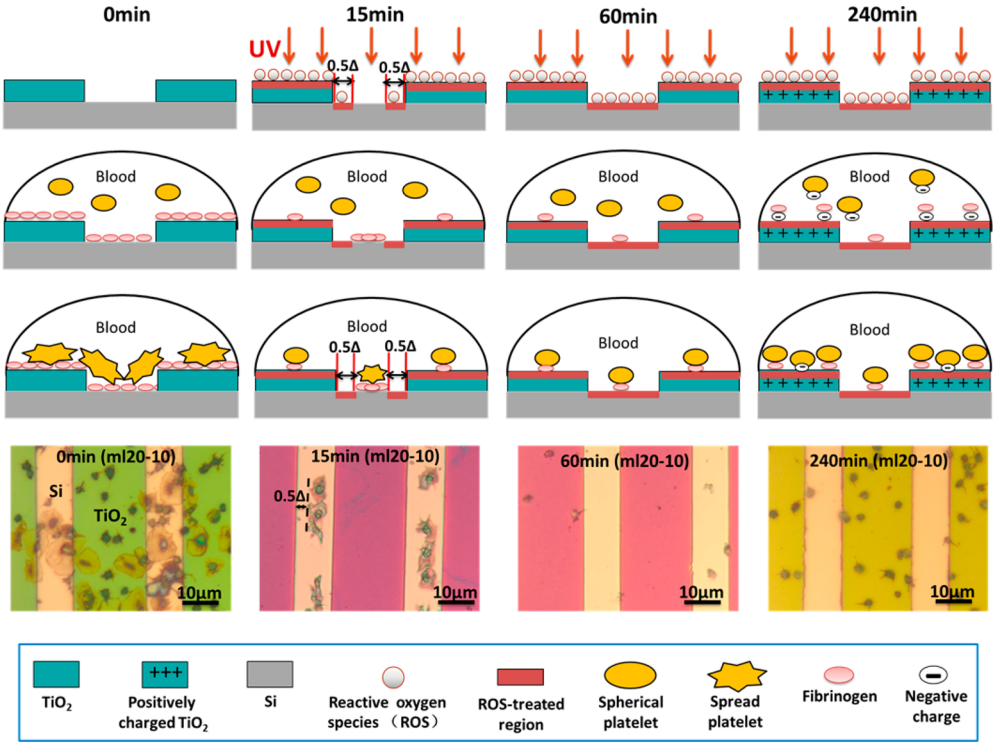

Figure 9. Proposed mechanism underlying the four representative types of platelets adhesion behavior on TiO_2−Si micropattern with various times of UV irradiation.

DOI: 10.1021/am509006y
ACS Appl. Mater. Interfaces 2015, 7, 4423−4432

micropattern, resulting in subsequent random adhesion and spreading of the platelets.

(2) The UV irradiation time was short (e.g., 15 min). The photogenerated ROS changed the nature of the TiO_2 region and diffused to the nearby Si region to change its nature. When in contact with the blood, the fibrinogen was selectively adsorbed to the inner of the Si region, which, in the absence of the treatment of ROS, subsequently resulted in the selective adhesion and spreading of platelets.

(3) The duration of UV irradiation was relatively long (e.g., 60 min). The photogenerated ROS changed the nature of the entire surface of the TiO_2−Si micropattern, which suppressed the fibrinogen adsorption and subsequent platelet adhesion.

(4) The UV irradiation time was long enough (e.g., 240 min). The photogenerated ROS changed the nature of the entire TiO_2−Si surface to suppress the fibrinogen adsorption and platelet adhesion. The photogenerated ROS can also clean the surface, which may cause an increase of the positive charge, and thus may relatively improve by electrostatic attraction the attachment of the negatively charged fibrinogen and platelets.[6,7] It should be noted that platelet spreading was inhibited. This result indicates that after 240 min of UV irradiation, the suppression effect was the main effect of the TiO_2 films on platelet adhesion, and not the enhancement one.

4. CONCLUSION

Model 1 and three other models indicated that photogenerated ROS and ROS-induced surface changes were related to the improvement in the anticoagulant properties of anatase TiO_2 films. Moreover, from model 2−4, it can be concluded that the TiO_2 films behave like an anticoagulant material whose properties change depending on the duration of UV irradiation. This is a schematic of the presented results:

(1) A short time (e.g., 1 min) of UV irradiation provides the TiO_2 surface with the suppression effect. It seems like the suppression effect is not mainly caused by the photoinduced superhydrophilicity, increased −OH groups, nor the decomposition of the adsorbed hydrocarbon. However, the underlying mechanism of the suppression effect needs further investigation (model 2 and model 3).

(2) The suppression effect of UV-irradiated TiO_2 films on fibrinogen adsorption and platelet adhesion extended from the UV-irradiated TiO_2 surface to the nearby masked TiO_2 or Si surfaces with increasing UV irradiation time. The results support that the suppression effect could be related to the change of TiO_2 that is further caused by the photogenerated and diffused ROS. Moreover, it indicates that the photogenerated ROS of the TiO_2 films could be used to improve the anticoagulant properties of the nearby materials (e.g., Si; models 3 and 4).

(3) A long time (e.g., 240 min) of UV irradiation seems likely to provided TiO_2 surface with the enhancement effect on fibrinogen adsorption and platelet adhesion. This could be related to the decomposition of adsorbed hydrocarbon and the positive change increase. However, in comparison with the enhancement effect, the suppression effect was the main effect of the TiO_2 films on the fibrinogen adsorption and platelet adhesion (models 2−4).

■ ASSOCIATED CONTENT

Supporting Information

Experimental parameters of deposition of the TiO_2 films and fabrication process of the TiO_2−Si micropattern. This material is available free of charge via the Internet at http://pubs.acs.org.

■ AUTHOR INFORMATION

Corresponding Author

*E-mail: yangping8@263.net.

Notes

The authors declare no competing financial interest.

■ ACKNOWLEDGMENTS

The authors would like to thank Dr. Ansha Zhao, Dr. Zhilu Yang, and Dr. Si Chen for their help and valuable discussions. This study was supported by the Key Basic Research Project (No. 2011CB606204), the National Natural Science Foundation of China (No. 30870629), and The Sichuan Youth Science & Technology Foundation (No. 2012JQ0001) for Distinguished Young Scholars.

■ REFERENCES

(1) Nan, H.; Ping, Y.; Xuan, C.; Yongxang, L.; Xiaolan, Z.; Guangjun, C.; Zihong, Z.; Feng, Z.; Yuanru, C.; Xianghuai, L.; Tingfei, X. Blood Compatibility of Amorphous Titanium Oxide Films Synthesized by Ion Beam Enhanced Deposition. *Biomaterials* **1998**, *19*, 771−776.

(2) Sul, Y.-T.; Johansson, C. B.; Petronis, S.; Krozer, A.; Jeong, Y.; Wennerberg, A.; Albrektsson, T. Characteristics of the Surface Oxides on Turned and Electrochemically Oxidized Pure Titanium Implants up to Dielectric Breakdown: The Oxide Thickness, Micropore Configurations, Surface Roughness, Crystal Structure, and Chemical Composition. *Biomaterials* **2002**, *23*, 491−501.

(3) Chen, J.; Zhao, A.; Chen, H.; Liao, Y.; Yang, P.; Sun, H.; Huang, N. The Effect of Full/Partial UV-Irradiation of TiO_2 Films on Altering the Behavior of Fibrinogen and Platelets. *Colloids Surf., B* **2014**, *122*, 709−718.

(4) Sawase, T.; Jimbo, R.; Baba, K.; Shibata, Y.; Ikeda, T.; Atsuta, M. Photo-induced Hydrophilicity Enhances Initial Cell Behavior and Early Bone Apposition. *Clin. Oral Implants Res.* **2008**, *19*, 491−496.

(5) Aita, H.; Hori, N.; Takeuchi, M.; Suzuki, T.; Yamada, M.; Anpo, M.; Ogawa, T. The Effect of Ultraviolet Functionalization of Titanium on Integration with Bone. *Biomaterials* **2009**, *30*, 1015−1025.

(6) Iwasa, F.; Hori, N.; Ueno, T.; Minamikawa, H.; Yamada, M.; Ogawa, T. Enhancement of Osteoblast Adhesion to UV-photofunctionalized Titanium via an Electrostatic Mechanism. *Biomaterials* **2010**, *31*, 2717−2727.

(7) Hori, N.; Ueno, T.; Minamikawa, H.; Iwasa, F.; Yoshino, F.; Kimoto, K.; Lee, M. C.-I.; Ogawa, T. Electrostatic Control of Protein Adsorption on UV-photofunctionalized Titanium. *Acta Biomater.* **2010**, *6*, 4175−4180.

(8) Kawahara, K.; Ohko, Y.; Tatsuma, T.; Fujishima, A. Surface Diffusion Behavior of Photo-generated Active Species or Holes on TiO_2 Photocatalysts. *Phys. Chem. Chem. Phys.* **2003**, *5*, 4764−4766.

(9) Lee, M. C.; Choi, W. Solid Phase Photocatalytic Reaction on the Soot/TiO_2 Interface: The Role of Migrating OH Radicals. *J. Phys. Chem. B* **2002**, *106*, 11818−11822.

(10) George, S.; Pokhrel, S.; Ji, Z.; Henderson, B. L.; Xia, T.; Li, L.; Zink, J. I.; Nel, A. E.; Mädler, L. Role of Fe Doping in Tuning the Band Gap of TiO_2 for the Photo-Oxidation-Induced Cytotoxicity Paradigm. *J. Am. Chem. Soc.* **2011**, *133*, 11270−11278.

(11) Yamakata, A.; Ishibashi, T.-a.; Onishi, H. Water- and Oxygen-Induced Decay Kinetics of Photogenerated Electrons in TiO_2 and Pt/TiO_2: A Time-Resolved Infrared Absorption Study. *J. Phys. Chem. B* **2001**, *105*, 7258−7262.

(12) Yoshihara, T.; Katoh, R.; Furube, A.; Tamaki, Y.; Murai, M.; Hara, K.; Murata, S.; Arakawa, H.; Tachiya, M. Identification of

DOI: 10.1021/am509006y
ACS Appl. Mater. Interfaces 2015, 7, 4423−4432

Reactive Species in Photoexcited Nanocrystalline TiO_2 Films by Wide-Wavelength-Range (400−2500 nm) Transient Absorption Spectroscopy. *J. Phys. Chem. B* **2004**, *108*, 3817−3823.
(13) Krötz, F.; Sohn, H. Y.; Gloe, T.; Zahler, S.; Riexinger, T.; Schiele, T. M.; Becker, B. F.; Theisen, K.; Klauss, V.; Pohl, U. NAD(P)H Oxidase−dependent Platelet Superoxide Anion Release Increases Platelet Recruitment. *Blood* **2002**, *100*, 917−924.
(14) Wachowicz, B.; Olas, B.; Zbikowska, H. M.; Buczyński, A. Generation of Reactive Oxygen Species in Blood Platelets. *Platelets* **2002**, *13*, 175−182.
(15) Stief, T. W.; Kurz, J.; Doss, M. O.; Fareed, J. Singlet Oxygen Inactivates Fibrinogen, Factor V, Factor VIII, Factor X, and Platelet Aggregation of Human Blood. *Thromb. Res.* **2000**, *97*, 473−480.
(16) Belisario, M. A.; Tafuri, S.; Di Domenico, C.; Squillacioti, C.; Della Morte, R.; Lucisano, A.; Staiano, N. H_2O_2 Activity on Platelet Adhesion to Fibrinogen and Protein Tyrosine Phosphorylation. *Biochim. Biophys. Acta, Mol. Cell Res.* **2000**, *1495*, 183−193.
(17) Ishibashi, K.-I.; Fujishima, A.; Watanabe, T.; Hashimoto, K. Generation and Deactivation Processes of Superoxide Formed on TiO_2 Film Illuminated by Very Weak UV Light in Air or Water. *J. Phys. Chem. B* **2000**, *104*, 4934−4938.
(18) Heard, D. E.; Pilling, M. J. Measurement of OH and HO_2 in the Troposphere. *Chem. Rev.* **2003**, *103*, 5163−5198.
(19) Morin, S.; Sander, R.; Savarino, J. Simulation of the Diurnal Variations of the Oxygen Isotope Anomaly ($\Delta^{17}O$) of Reactive Atmospheric Species. *Atmos. Chem. Phys.* **2011**, *11*, 3653−3671.
(20) Att, W.; Hori, N.; Takeuchi, M.; Ouyang, J.; Yang, Y.; Anpo, M.; Ogawa, T. Time-Dependent Degradation of Titanium Osteoconductivity: An Implication of Biological Aging of Implant Materials. *Biomaterials* **2009**, *30*, 5352−5363.
(21) Mattsson, A.; Österlund, L. Adsorption and Photoinduced Decomposition of Acetone and Acetic Acid on Anatase, Brookite, and Rutile TiO_2 Nanoparticles. *J. Phys. Chem. C* **2010**, *114*, 14121−14132.
(22) Wang, R.; Hashimoto, K.; Fujishima, A.; Chikuni, M.; Kojima, E.; Kitamura, A.; Shimohigoshi, M.; Watanabe, T. Light-Induced Amphiphilic Surfaces. *Nature* **1997**, *388*, 431−432.
(23) Gao, Y.; Masuda, Y.; Koumoto, K. Light-Excited Superhydrophilicity of Amorphous TiO_2 Thin Films Deposited in an Aqueous Peroxotitanate Solution. *Langmuir* **2004**, *20*, 3188−3194.
(24) Wang, R.; Sakai, N.; Fujishima, A.; Watanabe, T.; Hashimoto, K. Studies of Surface Wettability Conversion on TiO_2 Single-Crystal Surfaces. *J. Phys. Chem. B* **1999**, *103*, 2188−2194.
(25) Gray, J. J. The Interaction of Proteins with Solid Surfaces. *Curr. Opin. Struct. Biol.* **2004**, *14*, 110−115.
(26) Ohtsu, N.; Masahashi, N.; Mizukoshi, Y.; Wagatsuma, K. Hydrocarbon Decomposition on a Hydrophilic TiO_2 Surface by UV Irradiation: Spectral and Quantitative Analysis Using in Situ XPS Technique. *Langmuir* **2009**, *25*, 11586−11591.
(27) Sakai, N.; Fujishima, A.; Watanabe, T.; Hashimoto, K. Quantitative Evaluation of the Photoinduced Hydrophilic Conversion Properties of TiO_2 Thin Film Surfaces by the Reciprocal of Contact Angle. *J. Phys. Chem. B* **2003**, *107*, 1028−1035.
(28) Thevenot, P.; Hu, W.; Tang, L. Surface Chemistry Influence Implant Biocompatibility. *Curr. Top. Med. Chem.* **2008**, *8*, 270−80.
(29) Zhang, D. Chemical Synthesis of Ni/TiO_2 Nanophotocatalyst for UV/Visible Light Assisted Degradation of Organic Dye in Aqueous Solution. *J. Sol−Gel Sci. Technol.* **2011**, *58*, 312−318.
(30) Haick, H.; Paz, Y. Long-Range Effects of Noble Metals on the Photocatalytic Properties of Titanium Dioxide. *J. Phys. Chem. B* **2003**, *107*, 2319−2326.
(31) Corum, L. E.; Hlady, V. The Effect of Upstream Platelet−fibrinogen Interactions on Downstream Adhesion and Activation. *Biomaterials* **2012**, *33*, 1255−1260.
(32) Li, J.; Zhang, K.; Yang, P.; Liao, Y.; Wu, L.; Chen, J.; Zhao, A.; Li, G.; Huang, N. Research of Smooth Muscle Cells Response to Fluid Flow Shear Stress by Hyaluronic Acid Micro-Pattern on a Titanium Surface. *Exp. Cell Res.* **2013**, *319*, 2663−2672.
(33) Li, G.; Zhao, X.; Zhao, W.; Zhang, L.; Wang, C.; Jiang, M.; Gu, X.; Yang, Y. Porous Chitosan Scaffolds with Surface Micropatterning and Inner Porosity and Their Effects on Schwann Cells. *Biomaterials* **2014**, *35*, 8503−8513.
(34) Tatsuma, T.; Tachibana, S.-I.; Miwa, T.; Tryk, D. A.; Fujishima, A. Remote Bleaching of Methylene Blue by UV-Irradiated TiO_2 in the Gas Phase. *J. Phys. Chem. B* **1999**, *103*, 8033−8035.
(35) Zou, J.; Gao, J.; Wang, Y. Synthesis of Highly Active H_2O_2-Sensitized Sulfated Titania Nanoparticles with a Response to Visible Light. *J. Photochem. Photobiol., A* **2009**, *202*, 128−135.
(36) Tojo, S.; Tachikawa, T.; Fujitsuka, M.; Majima, T. Iodine-Doped TiO_2 Photocatalysts: Correlation between Band Structure and Mechanism. *J. Phys. Chem. C* **2008**, *112*, 14948−14954.
(37) Aita, H.; Att, W.; Ueno, T.; Yamada, M.; Hori, N.; Iwasa, F.; Tsukimura, N.; Ogawa, T. Ultraviolet Light-Mediated Photofunctionalization of Titanium to Promote Human Mesenchymal Stem Cell Migration, Attachment, Proliferation, and Differentiation. *Acta Biomater.* **2009**, *5*, 3247−3257.
(38) Tulloch, A. W.; Chun, Y.; Levi, D. S.; Mohanchandra, K. P.; Carman, G. P.; Lawrence, P. F.; Rigberg, D. A. Super Hydrophilic Thin Film Nitinol Demonstrates Reduced Platelet Adhesion Compared with Commercially Available Endograft Materials. *J. Surg. Res.* **2011**, *171*, 317−322.
(39) Takemoto, S.; Yamamoto, T.; Tsuru, K.; Hayakawa, S.; Osaka, A.; Takashima, S. Platelet Adhesion on Titanium Oxide Gels: Effect of Surface Oxidation. *Biomaterials* **2004**, *25*, 3485−3492.
(40) Xiao, Q.; Ouyang, L. Photocatalytic Activity and Hydroxyl Radical Formation of Carbon-Doped TiO_2 Nanocrystalline: Effect of Calcination Temperature. *Chem. Eng. J.* **2009**, *148*, 248−253.
(41) Baek, M.-H.; Jung, W.-C.; Yoon, J.-W.; Hong, J.-S.; Lee, Y.-S.; Suh, J.-K. Preparation, Characterization and Photocatalytic Activity Evaluation of Micro- and Mesoporous TiO_2/Spherical Activated Carbon. *J. Ind. Eng. Chem.* **2013**, *19*, 469−477.
(42) Xing, M.; Shen, F.; Qiu, B.; Zhang, J. Highly-Dispersed Boron-Doped Graphene Nanosheets Loaded with TiO_2 Nanoparticles for Enhancing CO_2 Photoreduction. *Sci. Rep* **2014**, *4*, 6341−6347.
(43) Corum, L. E.; Eichinger, C. D.; Hsiao, T. W.; Hlady, V. Using Microcontact Printing of Fibrinogen to Control Surface-Induced Platelet Adhesion and Activation. *Langmuir* **2011**, *27*, 8316−8322.

DOI: 10.1021/am509006y
ACS Appl. Mater. Interfaces 2015, 7, 4423−4432